J Solid State Electrochem (2006) 10: 411–415
DOI 10.1007/s10008-005-0023-9

ORIGINAL PAPER

M. Y. Wu · J. M. Wang · J. Q. Zhang · C. N. Cao

Effects of coprecipitated manganese on the structure and electrochemical performance of Al-substituted α-nickel hydroxide

Received: 26 April 2005 / Revised: 12 May 2005 / Accepted: 25 May 2005 / Published online: 20 July 2005

Abstract The effects of manganese on the structure and electrochemical performance of Al-substituted α-$Ni(OH)_2$ prepared by a chemical co-precipitation method were studied. The results of XRD and IR showed that the Al-substituted $Ni(OH)_2$ with various Mn contents are typical α-phase. The Mn-free sample is labile in alkaline media and partly converted to β-$Ni(OH)_2$. The stability of the samples improves with the increase in Mn content. The results of galvanostatic charge-discharge experiments showed that the addition of Mn increases the difference between the oxygen evolution and charge potentials, which improves the charge efficiency and increases the discharge capacity. The Mn-containing samples display better cycle stability than the Ni/Al sample without Mn. The Al-substituted $Ni(OH)_2$ sample with Mn 9.3% shows the highest discharge capacity during the whole cycle, and the largest discharge capacity is 260 mAh g^{-1} .The electrochemical transfer resistance (R_t) value decreases with the increase of Mn content.

Keywords α-Nickel hydroxide · Nickel · Aluminum · Manganese · Electrochemical performance

Introduction

Nickel hydroxide is widely used as the positive electrode material in secondary alkaline nickel-based batteries. There are two phases in its reduced state known as α-$Ni(OH)_2$ and β-$Ni(OH)_2$, which transform to γ-NiOOH and β-NiOOH during charging, respectively. In commercial batteries, spherical β-$Ni(OH)_2$ is usually used as active materials since it has a high tapping density (>2.0 g cm^{-3}) and good stability in strong alkaline electrolyte. However, β-$Ni(OH)_2$/β-NiOOH system has relatively low theoretical capacity and serious volume expansion after extended overcharge [1], which limit the further improvement on the performance of the nickel-based batteries.

For α-$Ni(OH)_2$/γ-NiOOH system, large discharge capacity can be obtained since the oxidation state of nickel in γ-NiOOH is 3.67 or 3.3∼3.7 [2, 3], and there are no volume expansion and mechanical deformation problems. However, pure α-$Ni(OH)_2$ is very unstable in strong alkaline medium and easily transforms to the β-$Ni(OH)_2$ after a few electrochemical cycles. In order to prepare stable α-$Ni(OH)_2$, many studies have been carried out through partial substitution of nickel ion in the nickel hydroxide lattice by trivalent or divalent cations such as Al [4–8], Co [9, 10], Fe [11], Mn [12–15] and Zn [16, 17]. Among these metal elements, Al is the most attractive because of its high stability in trivalent state and cheapness. Kamath et al. [4] prepared the Al-substituted α-phase $Ni(OH)_2$ which was found to have prolonged stability in strongly alkaline medium when the Al contents ≥20% and increase the discharge potential.

The stabilized α-phase structure and high discharge potential can be obtained after adding Al^{3+} in the $Ni(OH)_2$ [4]. However, the oxygen evolution becomes easier and the difference between oxygen evolution and charge potentials becomes smaller due to the addition of Al^{3+}. This is unfavorable to improve the charge efficiency of the batteries. The addition of Mn is an effective method for improving the conductivity of the active material and increasing the oxygen evolution potential [14, 15].

Although the Al-substituted $Ni(OH)_2$ have been investigated in their synthesis, structural characterization and electrochemical performance, the effects of Mn

M. Y. Wu · J. M. Wang (✉) · J. Q. Zhang · C. N. Cao
Department of Chemistry, Zhejiang University,
Hangzhou, 310027, People's Republic of China
E-mail: wjm@cmsce.zju.edu.cn.
Tel.: +86-571-87951513
Fax: +86-571-87951895.

J. Q. Zhang · C. N. Cao
State Key Laboratory for Corrosion and Protection,
Shenyang, 110015 People's Republic of China

on the performance of the Al-substituted $Ni(OH)_2$ have not been studied [4, 6]. In this paper, the effects of Mn on the physical properties and electrochemical performance of the Al-substituted $Ni(OH)_2$ prepared by a chemical co-precipitation method are investigated in detail.

Experimental

Preparation of samples

NaOH solution (2 M) and the mixed solution consisting of a required mole ratio of $NiSO_4$, $MnSO_4$, $Al_2(SO_4)_3$ and excess H_2O_2 were slowly added to a well-sealed reaction vessel with 250 cm^3 aqueous ammonia solution (pH = 10.0) at the same feeding speed under vigorous stirring. Reaction temperature was controlled at 50 ± 1 °C, and the pH value of reaction solution was held at 10.0 ± 0.1. After finishing the precipitation reaction, the reaction product was aged in the mother solution for another 15 h at 50 °C. The product was filtered off, washed several times with deionized water to neutral, and dried at 60 °C in air.

Characterization of samples

The structures of the samples were determined using X-ray diffractometer (Rigaku D/Max 2550), Cu Kα radiation at 40 kV, 300 mA, and a scanning rate of 8° (2θ) min^{-1}. The infrared spectroscopy of the samples was performed using a Nicolet Nexus 670 Fourier transform infrared (FTIR) spectrophotometer. The chemical compositions (Ni, Al and Mn contents) of the samples were obtained using an atomic absorption spectrophotometer (AAS) (model 180–50 from Hitachi). The content of SO_4^{2-} was determined by chemical analysis.

The pasted nickel electrodes were prepared as follows: 90 wt.% sample, 5 wt.% cobalt powder and 5 wt.% graphite powder were thoroughly mixed with a certain amount of 5% PTFE solution. The paste obtained was incorporated into nickel foam (2 cm×2 cm× 0.9 mm) with a spatula. The pasted nickel electrodes were dried at 50 °C and then roll-pressed to a thickness of 0.5 mm. Thereafter, the electrodes were soaked in 6 M KOH solution for 24 h before being coupled with porous Ni electrodes on either side as counters and a Hg/HgO electrode as reference. Galvanostatic charge-discharge studies were conducted using a DC-5 cell performance-testing instrument (Zhengfang Electron Appliance Company, Shanghai, China). The working electrode was galvanostatically charged at 0.1 C rate for 15 h, rest for 5 min, and then discharged to 0.1 V versus Hg/HgO at 0.1 C rate for 4 activation cycles. Cycle performance was tested under the following scheme: charge at 1.0 C rate for 1.3 h, rest for 5 min, and discharge at 1.0 C rate to 0.1 V versus Hg/HgO. Electrochemical impedance spectroscopy (EIS) measurements were performed by Potentiosta/Galvanostat Model 273A (Princeton Applied Research, USA) in conjunction with a model 5210 lock-in amplifier (Princeton Applied Research). In EIS measurements the range of frequency was between 0.005 Hz and 120 kHz, and the excitation amplitude was 10 mV.

Results and discussion

Structure and stability of the samples

In all the samples prepared, the mole ratio of Al to (Ni + Al + Mn) is almost kept at 10%, and the samples with various Mn contents are designated as Mn C%, where C% is the mole percentage of Mn versus the total amount of Ni, Al and Mn.

The chemical compositions of the samples are presented in Table 1. It can be seen that the Al content in various samples has little change, and the Ni content decreases with the increase of the Mn content. It is also noted that the SO_4^{2-} content in the samples obviously increases with the increase of the Mn content.

The powder X-ray diffraction (XRD) patterns of the Al-substituted $Ni(OH)_2$ sample with various manganese contents are shown in Fig. 1. The Mn-free sample shows mainly α-phase, as well as a small percentage of β-phase, which is caused by relatively lower Al content [4]. The Al-substituted $Ni(OH)_2$ samples with manganese show

Table 1 The chemical composition of nickel hydroxide samples

Sample	Ni (mole%)	Al (mole%)	Mn (mole%)	SO_4^{2-} (wt.%)
1	89.9	10.1	0.0	5.5
2	84.8	10.4	4.8	7.8
3	79.7	11.0	9.3	9.8
4	75.3	10.8	13.9	13.4

The mole % relates to the overall content of the three metals

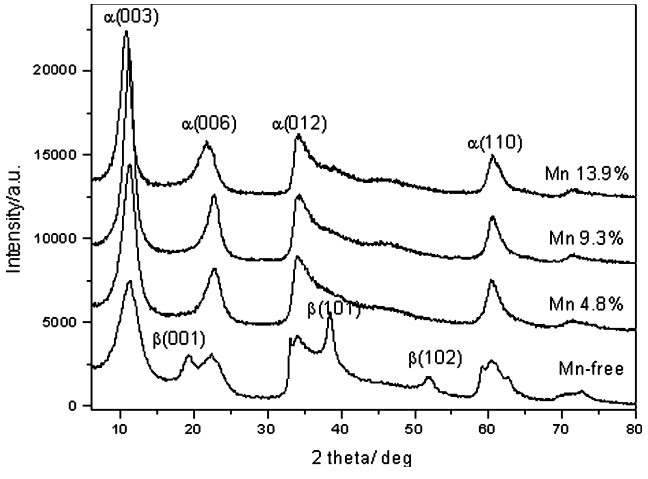

Fig. 1 XRD patterns of the Al-substituted nickel hydroxide with various manganese contents

typical α-phase peaks. The patterns are similar to the standard XRD pattern of α-$3Ni(OH)_2{\cdot}2H_2O$ (JCPDS 22–444). The first two peaks at 11 and 23° correspond to the (003) and (006) planes, respectively.

The infrared spectra of the Al-substituted $Ni(OH)_2$ samples with various manganese contents are shown in Fig. 2. The three Al-substituted $Ni(OH)_2$ samples with various manganese contents (Mn 4.8∼13.9%) show the characteristics of α-$Ni(OH)_2$. The broad peak at about 3,450 cm^{-1} is characteristic of the stretching vibration of hydroxyl groups hydrogen-bonded to H_2O, and the band at 1,630 cm^{-1} corresponds to the bending mode of water molecules. The disappearance of the narrow band at 3,650 cm^{-1} suggests that the OH groups are not free but hydrogen bonded with the water molecules present in the interslab space. The band close to 1,100 cm^{-1} and a shoulder at 620 cm^{-1} are due to free SO_4^{2-} ions, which originate from the metal salt solution used for the precipitation [11, 18]. But for Mn-free sample, there is a 3,650 cm^{-1} weak peak, which results from a small percentage of β-phase existence in sample. These results are in good agreement with those of XRD.

In order to investigate the stability of the samples in strongly alkaline medium, the samples with different Mn contents were aged in 6 M KOH solution at room temperature for 30 days. Their XRD patterns are shown in Fig. 3. Several peaks at 19, 33, 38, 52, 59 and 62°, indicative of β-$Ni(OH)_2$ separate obviously from α-phase in the XRD patterns of the Mn-free sample, which indicates that one part of α-phase transforms into β-phase. The Mn 9.3% and Mn 13.9% samples retain the α-phase and the peaks become sharper and stronger after the ageing treatment for 30 days, which indicates that their crystallinity has improved. However, two small peaks at about 19 and 38° appear in the Mn 4.8% sample, which is the characteristic of β-$Ni(OH)_2$. The preceding results of chemical analyses (Table 1) show that the samples with larger Mn contents have higher

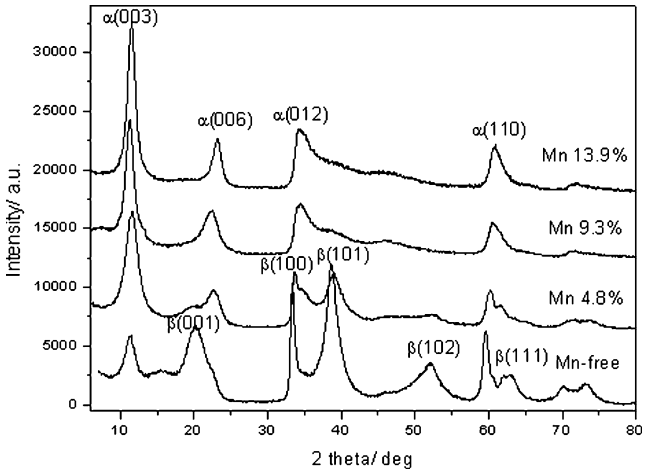

Fig. 3 XRD patterns of the Al-substituted nickel hydroxide with various manganese contents after ageing for 30 days at room temperature in 6 M KOH

SO_4^{2-} contents to compensate for the excess of positive charges caused by the introduction of Al^{3+} and Mn^{3+}, which can enhance the structural stability of α-$Ni(OH)_2$ [11]. Therefore, the addition of Mn improves the structural stability of the Al-substituted α-$Ni(OH)_2$ in the alkaline medium, and the samples with larger Mn contents display better stability.

Electrochemical performance of samples

Figure 4 shows the fourth charge-discharge curves of the Al-substituted $Ni(OH)_2$ samples with various manganese contents at 1.0 C rate. The specific capacity is in terms of the capacity per gram of sample. The Al-substituted $Ni(OH)_2$ samples with Mn display a flat discharge plateau. While the potential of the samples slowly increases during the charging process and finally reaches a plateau

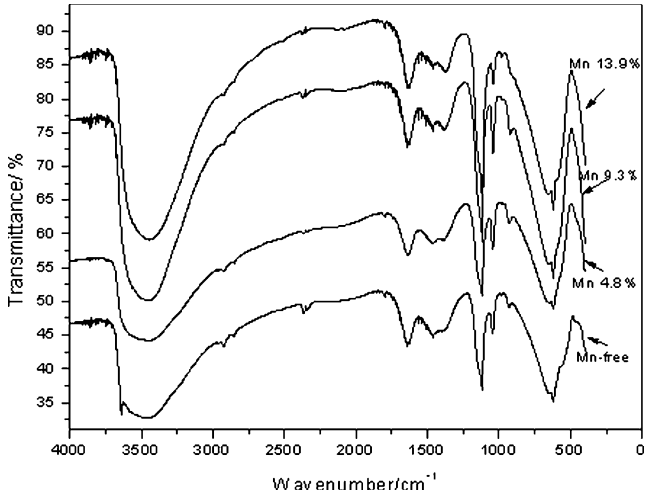

Fig. 2 IR patterns of the Al-substituted nickel hydroxide with various manganese contents

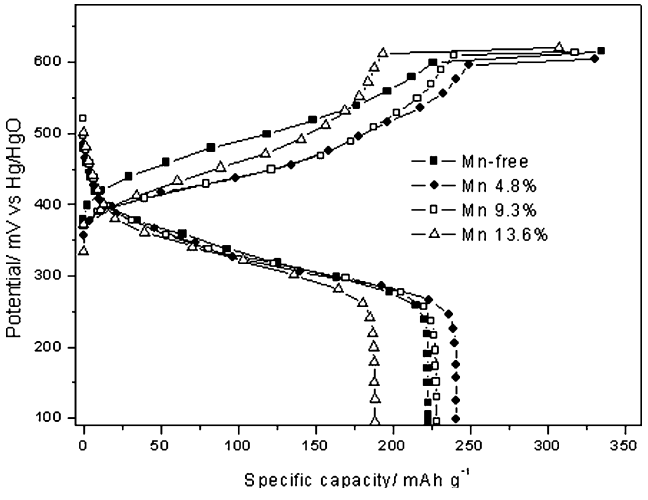

Fig. 4 The charge-discharge curves of the Al-substituted nickel hydroxide with various manganese contents

Table 2 Data from the charge-discharge curves of the Al-substituted nickel hydroxide with various manganese contents at 1.0 C rate

Sample	E_{op} (mV)	E_{hd} (mV)	E_{hc} (mV)	E_{ox} (mV)	$E_{hc} - E_{hd}$ (mV)	$E_{ox} - E_{hc}$ (mV)
Mn-free	338	329	499	615	170	116
Mn 4.8%	289	315	450	605	135	155
Mn 9.3%	291	317	449	614	132	165
Mn 13.9%	297	327	454	621	127	167

that results from the evolution of oxygen. Table 2 shows the effects of Mn content on the open-circuit potential (E_{op}), the oxygen evolution potential (E_{ox}), half discharge potential (E_{hd}, defined as the potential at the half discharge capacity) and half charge potential (E_{hc}, defined as the potential at the half charge capacity before reaching the plateau of oxygen evolution) at 1.0 C rate. It can be noticed that the addition of Mn decreases the E_{op} of the electrodes at the discharged states, which is because Mn^{4+} has smaller size than Ni^{3+} [14]. E_{hd} decreases slightly and E_{hc} decreases markedly with the addition of Mn. The addition of Mn produces fewer effects on E_{ox}. The doping of Mn increases obviously the difference between E_{hc} and E_{ox} of the samples, which is advantageous for increasing the charging efficiency. It should be noted that the electrode polarization can be characterized by the (E_{hc} - E_{hd}) value, and larger (E_{hc} - E_{hd}) value implies higher electrode polarization. The data in Table 2 indicate that the addition of Mn decreases the electrode polarization, and the samples with large Mn contents have relatively low electrode polarization.

The cycle behavior of the Al-substituted $Ni(OH)_2$ with various manganese contents at 1.0 C rate is illustrated in Fig. 5, where NEE represents the number of electrons exchanged per Ni atom. The Mn-free sample displays a large capacity deterioration rate during the whole cycle, which may result from its instability in alkaline medium. The addition of Mn greatly improves the cycle stability of the Al-substituted $Ni(OH)_2$, and the NEE values of Mn 9.3% and Mn 13.9% samples even keep increasing during the whole cycle (300 cycles). The significant improvement on the cycle stability of the samples may be due to the fact that Mn^{3+} ions in the samples gradually transform into Mn^{4+} ions during the cycling process and the electrical conductivity of the samples in their discharge states increases [15]. The Mn 9.3% sample shows the largest NEE value during the whole electrochemical cycle. The discharge capacity of the Mn 13.9% sample is small in the initial stage of cycle experiment, then increases gradually and becomes larger than that of the Mn-free sample after 175 cycles, which indicates that the activation of the sample with larger Mn content is slow.

The electrochemical impedance spectra (EIS) of Al-substituted $Ni(OH)_2$ samples with various Mn contents after cycle experiment were measured at 100% DOD and the EIS are displayed in Fig. 6a.The model for the essential features of the electrode is represented by the electrical equivalent circuit shown in Fig. 6b, where R_s is the total ohmic resistance of the electrode, CPE is the constant phase element related to the double layer capacity, R_t the charge-transfer resistance of the electrode, W_o is the Generalized Finite Warburg impedance (Z_w) of the solid phase diffusion. The simulating results are tabulated in Table 3. It can be seen that both R_t and

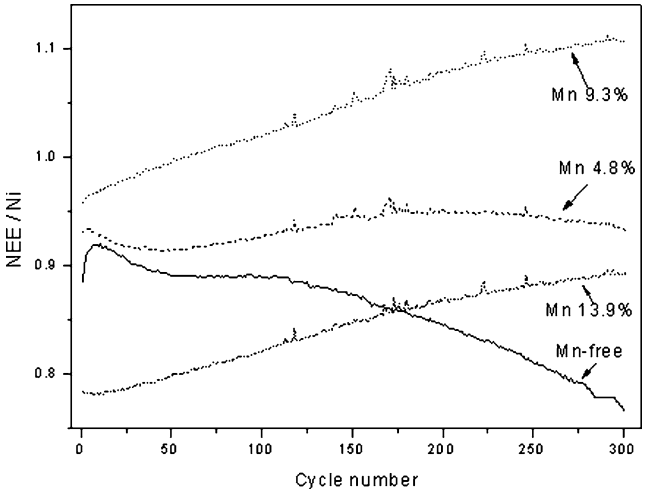

Fig. 5 The cycle performance of the Al-substituted $Ni(OH)_2$ with various manganese contents

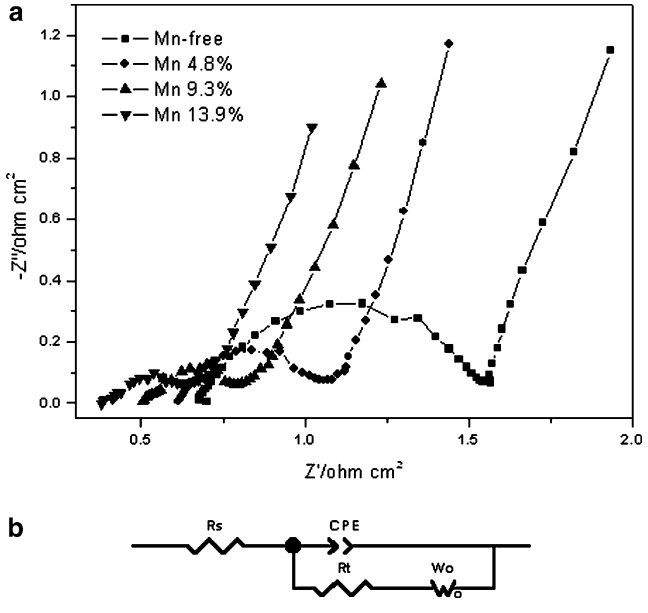

Fig. 6 Nyquist plots of the Al-substituted nickel hydroxide with various manganese contents (**a**) and equivalent circuit for nickel electrodes (**b**)

Table 3 Simulation results from EIS of the Al-substituted nickel hydroxide with various manganese contents

R_s is the total ohmic resistance of the electrode; R_t is the charge-transfer resistance of the electrode

Sample	R_t		R_s	
	Value/ohm cm^2	Error %	Value/ohm cm^2	Error %
Mn -free	3.00	0.71	3.05	0.36
Mn 4.8%	1.48	2.45	2.53	0.71
Mn 9.3%	0.85	4.38	2.13	0.83
Mn 13.9%	0.62	6.43	1.67	1.59

R_s decrease with the increase of Mn content, indicating that the doping of Mn in Al-substituted $Ni(OH)_2$ samples decreases ohmic and electrochemical polarizations of the electrodes, and this effect is enhanced with the increase of Mn content in the samples. This is in general agreement with the results of galvanostatic charge-discharge experiment.

Conclusions

1. The Al-substituted $Ni(OH)_2$ samples with various Mn contents were prepared by a coprecipitation method. The samples with Mn display typical α-phase, and the samples with larger Mn contents have better structural stability in strongly alkaline medium.
2. The doping of Mn improves the charging efficiency, cycle stability and discharge capacity of the Al-substituted $Ni(OH)_2$ electrodes. The sample with Mn 9.3% shows the highest discharge capacity during the whole electrochemical cycle, and its capacity reaches 260 mAh g^{-1} (the NEE is 1.1) at the 300th cycle.
3. The ohmic and electrochemical polarizations of the electrodes are markedly decreased by the doping of Mn in Al-substituted $Ni(OH)_2$, and the samples with larger Mn contents show lower electrode polarization.

Acknowledgements This work was supported by National Natural Science Foundation of China (Approval No. 59902004). The authors also gratefully acknowledge the financial support of the Chinese State Key Laboratory for Corrosion and Protection.

References

1. Bode H, Dehmelt K, Witte J (1966) Electrochim Acta 11:1079
2. Barnard R, Randell CF, Tye FF (1980) J Appl Electrochem 10:109
3. Corrigan DA, Knight SL (1989) J Electrochem Soc 136:613
4. Kamath PV, Dixit M, Indira L (1994) J Electrochem Soc 141:2956
5. Indira L, Dixit M, Kamath PV (1994) J Power Sources 52:93
6. Sugimoto A, Ishida S, Hanawa K (1999) J Electrochem Soc 146:1251
7. Zhang HB, Liu HS, Cao XJ, Li SJ, Sun CC (2003) Mater Chem Phys 79:37
8. Zhao YL, Wang JM, Chen H, Pan T, Zhang JQ, Cao CN (2004) Int J Hydrogen Energy 29:889
9. Faure C, Delmas C, Willmann P (1991) J Power Sources 36:497
10. Xie JY, Zhang QS, Liu JF, Shi PF (1999) Chin J Power Sources 23:238
11. Demourgues-Guerlon L, Delmas C (1993) J Power Sources 45:281
12. Demourgues-Guerlon L, Delmas C (1994) J Power Sources 52:269
13. Demourgues-Guerlon L, Delmas C (1994) J Power Sources 52:275
14. Demourgues-Guerlou L, Fournes L, Delmas C (1996) J Electrochem Soc 143:561
15. Axmann P, Glemser O (1997) J Alloys Compd 246:232
16. Dixit M, Kamath PV, Gopalakrishnan J (1999) J Electrochem Soc 146:79
17. Tessier C, Guerlou-Demourgues L, Faure C, Basterreix M, Nabias G, Delmas C (2000) Solid State Ionics 133:11
18. Faure C, Delmas C, Fouassier M (1991) J Power Sources 35: 279
19. Chen H, Wang JM, Pan T, Zhao YL, Zhang JQ, Cao CN (2003) J Electrochem Soc 150:1399